

## Study on the Theory and Simulation Experiment of Coal Gas Generation in Converter

Chen Fang<sup>1</sup>, Kang Xinlei<sup>2\*</sup>, Song Yingqian<sup>3\*</sup>, Qin Debo<sup>4</sup>, Xu Liang<sup>4</sup>, Zhang Chaojie<sup>2</sup> and Zhang Liqiang<sup>2\*</sup>

<sup>1</sup>Masteel Group Design and Research Institute Co., Ltd., Ma'anshan 243000, Anhui, China.

<sup>2</sup>School of Metallurgical Engineering, Anhui University of Technology, Ma'anshan 243032, Anhui, China.

<sup>3</sup>Steelmaking Plant, Yonggang Group Co., Ltd, Zhangjiagang 215628, Jiangsu, China.

<sup>4</sup>Anhui Changjiang Iron & Steel Co., Ltd, Ma'anshan 243000, Anhui, China.

**\*Corresponding Authors:** Kang Xinlei, Zhang Liqiang, Song Yingqian, Anhui University of Technology, Maanshan, Anhui, China; Song Yingqian, Steelmaking Plant, Yonggang Group Co., Ltd, Zhangjiagang, Jiangsu, China.

### ABSTRACT

In this paper, according to the three-stage theory of decarburization, the theoretical calculation of the gas volume of the main gas CO stirred converter bath generated in the decarburization process is carried out for the 120t converter with specific molten iron composition parameters. The theoretical equation of decarburization is deduced, and the carbon-oxygen reaction CO bubble physical simulation test device is designed. The hydraulic model in the laboratory is reduced according to the prototype 8:1 ratio. In this way, the accurate computer measurement of gas generation can be carried out, which provides theoretical support for actual production.

**Keywords:** Decarbonization; converter; carbon-oxygen reaction; simulation test.

### INTRODUCTION

With the proposal of 'carbon peak, carbon neutralization', the most rational recycling and utilization of energy should be carried out<sup>[1]</sup>. Iron and steel, known as 'industrial food', is an indispensable material for the development of national modernization. At present, high-efficiency smelting technology has become the core and key to the modern development of the iron and steel industry. Converter steelmaking is the main method in China, which accounts for about 90%<sup>[2-4]</sup>. The decarburization reaction is a major reaction throughout the whole blowing process of converter smelting. In the smelting process, the carbon-oxygen reaction in the molten pool generates a large number of bubbles to form a strong stirring of the molten steel, which promotes the chemical reaction rate, uniform composition and temperature of the steel-slag interface. The amount of bubbles generated by the carbon-oxygen reaction in different decarburization stages is different, and the stirring ability of the molten pool is also different. Therefore, it is of great significance to accurately grasp the change of the amount of bubbles in the carbon-oxygen

reaction of the molten pool to study the mixing law of the molten pool.

Converter bath stirring is the core and foundation of the development of modern steelmaking technology, which is the key factor to determine the state and rate of metallurgical production process<sup>[5]</sup>. Mixing time ( $\tau$ ) is the most intuitive technical parameter to measure the mixing degree and solute diffusion rate of liquid stirring in converter bath. The length of mixing time has an important influence on the composition and temperature uniformity of molten steel in the bath, the elimination of inclusions and the increase of bath reaction rate<sup>[6]</sup>. Therefore, the research on the mixing time of liquid in the bath of the converter is to improve the mixing of the bath of the converter. Reasonable utilization and effective control of the stirring in the steelmaking process is of great significance for the efficient and stable smelting of the converter, and is the top priority of the efficient smelting of the modern converter. R. Guthrie<sup>[7-9]</sup> et al. pointed out that the steelmaking process is highly coupled with complex transmission phenomena, and numerical simulation is more economical

and time-saving. In this paper, the 120t converter is taken as the object. Considering the effect of CO bubbles generated by carbon-oxygen reaction in decarburization process on the stirring of molten pool, the model and scheme of simulation test are designed.

Through theoretical research, remarkable economic and environmental benefits are created for enterprises<sup>[10]</sup>.

### ESTABLISHMENT OF MACROKINETIC MATHEMATICAL MODEL OF CARBON-OXYGEN REACTION

The hydraulic model of the converter laboratory is reduced according to the prototype 8:1 ratio and is made of organic glass with a thickness of 10mm. The converter test model is shown in Figure 1.

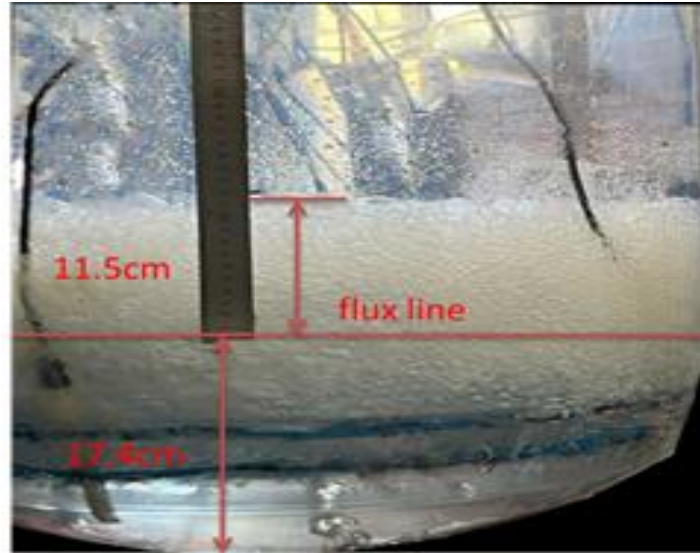
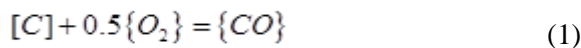


Figure1. Converter simulation test model and process diagram.

The molten iron is generally an alloy solution containing about 4% carbon and some other impurity elements. One of the main tasks of steel-making is decarburization. During the smelting process, a large number of bubbles generated by the carbon-oxygen reaction have sufficient stirring force to promote the bath stirring and increase the chemical reaction rate of the steel-slag interface. Relevant research shows that<sup>[11-14]</sup>, 55% of carbon is removed in the impact zone and 45% in the emulsification zone during the whole blowing period. In the later stage of converter blowing, the decarburization reaction in the circulating flow zone in the molten pool accounts for 30%~40% of the decarburization amount in the same period. At high temperature of converter, the main reactions of [C] in Converter as shown in formula (1)-(4).

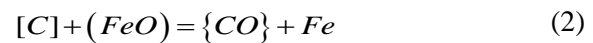
A part is directly oxidized at the gas-molten steel interface.



When the carbon content of the molten pool is high, CO<sub>2</sub> is also an oxidant, and the reaction of the following formula (2) will occur.



Part of [O] reacts with [O] in steel or slag, mainly at the slag- molten steel interface.



At high temperature, the oxidation product of [C] in the converter is mainly CO. It is generally believed that the gas contains about 90% CO and 10% CO<sub>2</sub>.

#### Basic Parameters of the Model

Taking the average composition of molten iron in 80 furnaces of 120 tons converter in a factory as the basic parameter, the molten iron and smelting composition are shown in Table 1.

Table1. 120t converter smelting process, raw materials and target composition parameters of a plant.

120t converter	oxygen flow / (Nm <sup>3</sup> ·h <sup>-1</sup> )	Scrap ratio / (%)	liquid iron	[C]	[Si]	[Mn]
				3%-5%	0.45%-0.55%	0.25%-0.35%
	20000~21000	17	liquid steel	C	Si	Mn
				0.12%	trace	0.1%

## Study on the Theory and Simulation Experiment of Coal Gas Generation in Converter

The hot metal contains 4%C, 0.5%Si, 0.3%Mn, and the scrap ratio is about 17%. The content of C, Mn and Si in the scrap is neglected. Molten steel  $\omega[C]=0.05\%$ ,  $\omega[Mn]=0.1\%$ ,  $\omega[Si]\approx\text{trace}$ . The actual top blowing flow rate of the converter in the steel plant is  $20000\sim 21000\text{ Nm}^3\cdot\text{h}^{-1}$ . In order to achieve the purpose of efficient smelting, this paper designs to increase the top blowing oxygen flow rate to  $21000\sim 23000\text{ Nm}^3\cdot\text{h}^{-1}$ , and takes the average top blowing oxygen flow rate to  $22000\text{ Nm}^3\cdot\text{h}^{-1}$  for model construction and calculation.

### Basic Assumptions

The oxidation product of [C] in converter furnace at high temperature is mainly CO. It is generally believed that the gas contains about 90%CO and about 10%CO<sub>2</sub>. The same amount of C is oxidized to produce the same amount of CO and CO<sub>2</sub>. In this paper, the influence of C-O reaction kinetics on the flow field behavior of molten pool is mainly studied. Therefore, in order to facilitate the establishment of the model, the following (1)-(4) assumptions are proposed.

- CO and CO<sub>2</sub> produced by carbon-oxygen reaction in converter have the same stirring effect on molten pool.
- The effect of temperature on the floating of carbon-oxygen reaction bubbles is not considered.

- Assuming that 85% of the carbon-oxygen reaction gas in the converter can effectively stir the molten pool, that is  $\alpha = 0.85$  ;
- Other chemical reactions except carbon-oxygen reaction are not considered.

### Decarburization Theoretical Equation Derivation

The three-stage theory of decarburization in converter describes the decarburization law of molten pool in general, which can divide the change process of decarburization rate in oxygen converter into three stages: front, middle and back<sup>[15]</sup>. The low temperature in the early stage of decarburization is mainly due to the oxidation of silicon, and the decarburization reaction is inhibited. With the oxidation of silicon, the decarburization rate changes from slow to fast. In the middle stage of decarburization, the temperature of molten steel increases, and the decarburization rate is always maintained at the highest level. The 100% oxygen supplied is used for decarburization, and the decarburization rate is almost only determined by the oxygen supply intensity. The reaction continues in the later stage of decarburization, but the carbon concentration in the steel is very low at this time, and the decarburization rate decreases with the decrease of carbon content in the molten steel. The curve of decarburization rate change during the whole decarburization process is called 'step curve', as shown in Fig.2.

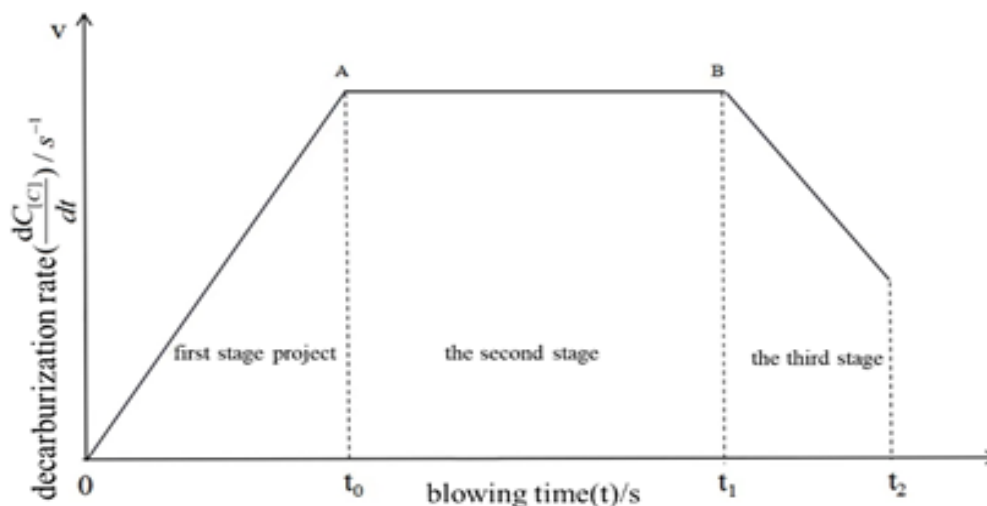


Figure2. Classical decarburization three-stage theory diagram.

The differential form of decarburization rate before, during and after converter smelting is shown in the following (5)-(7) formulas.

$$-\frac{dC}{dt} = K_1 t + m \quad (4)$$

$$-\frac{dC}{dt} = K_2 \quad (5)$$

$$-\frac{dC}{dt} = K_3 \omega_c \quad (6)$$

In the formula:  $-\frac{dC}{dt}$  -Decarburization rate,  $\%(C) \cdot \text{min}^{-1}$

$m$  -constant, which is used to describe the

decarbonization rate of oxygen blowing;

$K_1$ -The first decarburization reaction rate constant;

$t$ -Oxygen blowing time of converter, min;

$K_2$ -The second stage decarburization reaction rate constant;

$K_3$ -The third stage decarburization reaction rate constant;

$\omega_C$ -Carbon content of molten steel in converter bath, %.

The carbon content change function of each stage can be obtained by integrating the decarburization rate equation as shown in the (8)-(10) formula.

$$\omega_C = \omega_{C_0} - \frac{1}{2} K_1 t^2 - m \quad 0 \leq t \leq t_1 \quad (7)$$

$$\omega_C = \omega_{C_A} - K_2 t \quad t_1 \leq t \leq t_2 \quad (8)$$

$$\omega_C = \omega_{C_B} \cdot e^{-K_3 t} \quad t_2 \leq t \leq t_3 \quad (9)$$

In the formula:

$\omega_C$  -Decarbonization rate, % (C) · min<sup>-1</sup>;

$\omega_{C_0}$  -Initial carbon content of molten pool, %;

$\omega_{C_A}$  -The carbon content of the molten pool at the turning point before and during decarburization, %;

$\omega_{C_B}$  -The carbon content of the turning point molten pool in the middle and late stage of decarburization, %;

$t_1$ -Oxygen blowing time at the turning point before and during decarburization of converter,min;

$t_2$ -Oxygen blowing time at the turning point in the middle and late stage of converter decarburization. min;

$t_3$ -Oxygen blowing time at the end of converter blowing, min.

In the early stage of decarburization reaction, the reactant concentration has little effect on the decarburization rate, and this stage is not a restrictive link. In the middle stage of decarburization reaction, the decarburization rate only depends on the oxygen supply intensity. Under the condition of sufficient oxygen supply, the decarburization rate remains almost unchanged at a high level, and the mass transfer

at this stage does not become a limiting link. The diffusion of the third stage of decarburization is the most important limiting step in the later stage of converter blowing, and the decarburization reaction rate is affected by the [C] diffusion rate.

### Phase II Decarburization Rate Equation

The second stage decarburization rate  $v_2$  is proportional to the oxygen flow  $F_{O_2}$ , Therefore, the second stage rate equation is shown in (11)-(13).

$$v_2 = -\frac{W}{100} \frac{d\omega_C}{dt} = k_2 F_{O_2} \quad (10)$$

$$k_2 = \eta_{O_2} \times m_C \quad (11)$$

$$v_2 = -\frac{d\omega_C}{dt} = \frac{100\eta_{O_2} m_C F_{O_2}}{W} \quad (12)$$

In the formula:

$W$  -Converter loading metal weight, kg;

$k_2$  -The mass of effective oxygen oxidizable carbon per cubic meter in standard state,  $kg \cdot m^{-3}$ ;

$\eta_{O_2}$  -Effective utilization rate of oxygen;

$m_C$  -Mass of oxidisable carbon per cubic meter of oxygen in standard state, kg;

$F_{O_2}$  -Top blowing oxygen flow,  $Nm^3 \cdot h^{-1}$ .

### Phase I Decarburization Rate

The decarburization reaction rate  $v_1$  in the first stage of decarburization is affected by the temperature, Si and Mn of the molten iron blowing process.

The derivation process of the first stage decarburization rate  $v_1$  is shown below.

The oxygen consumption of C, Si, Mn and FeO at the end of stage I is shown in Formula (14).

$$Q_1 = \left[ (\omega_{C_0} - \omega_{C_A}) + (\omega_{Si_0} - \omega_{Si_m}) + (\omega_{Mn_0} - \omega_{Mn_m}) + \omega_{FeO} \right] \times q_i \quad (13)$$

According to the oxygen supply intensity of top blowing and the amount of molten iron, the end time  $t_1$  of the first stage of decarburization was obtained.

$$t_1 = \frac{Q_1 T_1}{\eta_{O_2} F_{O_2}} \quad (14)$$

At the end of the first stage of decarburization, the carbon content of the molten pool  $\omega_{C_A}$  at the turning point of the first and second stages and the turning time  $t_1$ , so the constant  $K_1$  and  $m$  can

## Study on the Theory and Simulation Experiment of Coal Gas Generation in Converter

be obtained by solving the equation (6) and then the decarburization rate  $v_1$  of the first stage of decarburization can be obtained by simultaneous equation (5).

$$\begin{cases} \omega_{C_A} = \omega_{C_0} - \frac{1}{2} K_1 t_1^2 - m \\ v_2 = K_1 t_1 + m \end{cases} \quad (15)$$

In the formula:  $Q_1$  -Oxygen consumption per ton of molten iron,  $m^3 \cdot t^{-1}$ ;

$\omega_{Si_0}$  -Initial Si content of molten iron;

$\omega_{Si_m}$  -Target Si content in molten steel;

$\omega_{Mn_0}$  -Initial Mn content of molten iron;

$\omega_{Mn_m}$  -Mn content in target molten steel;

$\omega_{FeO}$  -FeO content in early slag;

$i$  -Material elements, C, Si, Mn, FeO;

$q_i$  -xygen consumption per ton of molten iron material element  $i$  in the standard state,  $m^3 \cdot t^{-1}$ ;

$T_l$  -he weight of molten iron in converter, t.

### Phase III Decarburization Rate

Because the carbon content at the turning point in the middle and late stages of decarburization is the same as the decarburization rate, there is the following formula (17).

$$K_3 = \frac{v_2}{\omega_{C_B}} \quad (16)$$

The late decarburization rate equation is Formula (18).

$$v_3 = -\frac{dC}{dt} = \frac{v_2}{\omega_{C_B}} \omega_C \quad (17)$$

### Carbon Content Curve of Each Stage

Substituting the fixed constants K1, K2, K3 and m obtained from the decarburization rate equation into Eq. (8), Eq. (9) and Eq. (10), the carbon content change functions of the three stages can be obtained respectively. Fig. 3 shows the curve of the carbon content of the molten pool with the blowing time.

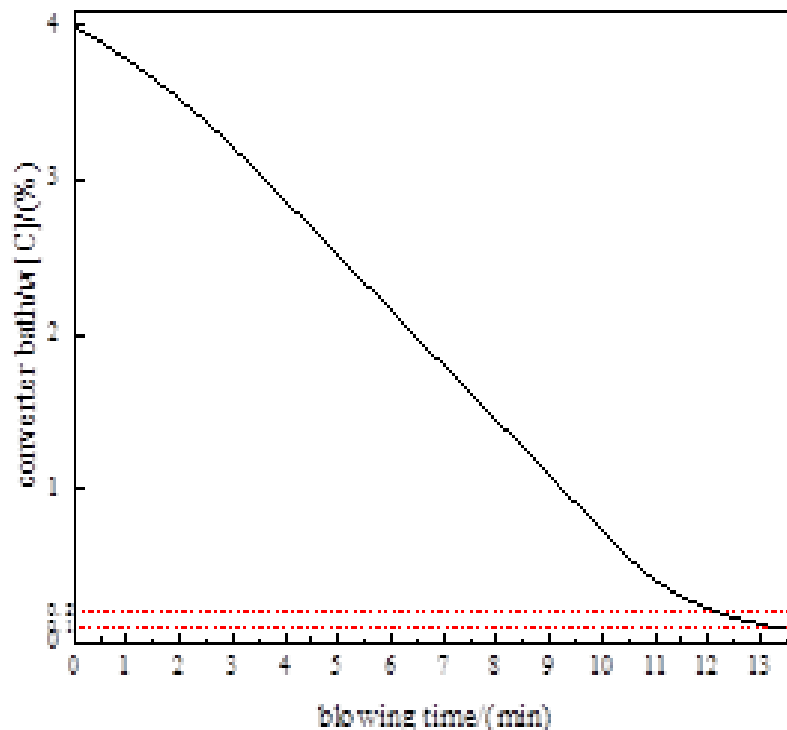


**Figure3.** Theoretical calculation of carbon content change curve in blowing process.

### Establishment of Mathematical Model

As the blowing time increases, the weight of molten iron in the converter gradually increases, and the variation of molten iron weight T with time in the molten pool can be seen in formula (19).

$$T = T_l + v_b t \quad (18)$$

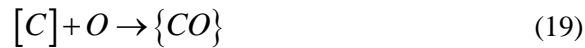
In the formula: T-eight of molten iron in converter bath, t;

$v_b$  - eight increase rate of converter semi-steel,  $t \cdot \min^{-1}$



## Study on the Theory and Simulation Experiment of Coal Gas Generation in Converter

According to the assumption that CO and CO<sub>2</sub> in the converter have the same stirring effect, therefore, the oxidation products of [C] in the converter can be written into formula (20).



For the determined weight and carbon content of molten iron in converter, according to the same molar amount of CO generated by the oxidation of [C] in Equation (20), the theoretical gas volume of CO generated by the oxidation of [C] in converter can be obtained. The instantaneous  $\Delta\omega_c$  in the converter bath is oxidized, and the theoretical instantaneous CO gas volume can be described as formula (21).

$$\frac{V_{CO}}{dt} = T \times 10^6 \times \frac{d\Delta\omega_c}{dt} \times \frac{22.4}{12} \times 10^{-3} \quad (20)$$

In the formula:

$V_{CO}$ -The amount of CO generated, m<sup>3</sup>;

$\Delta\omega_c$ -Variation of [C] in converter bath, %;

22.4-1mol gas volume in standard state, L;

12-The relative atomic mass of C.

Substituting the rate of each stage of the decarburization process into Formula (21), the theoretical instantaneous CO production of the

effective stirring of the molten pool in each stage before, during and after the decarburization of the converter can be obtained.

$$\left\{ \begin{array}{l} \text{prophase: } \left\{ \begin{array}{l} \frac{V_{CO}}{dt} = (T_1 + v_3 t) \times v_1 \times \frac{22.4}{12} \times 10^3 \times 60 \times \alpha \\ \frac{V_{CO}}{dt} = (T_1 + v_3 t) \times v_2 \times \frac{22.4}{12} \times 10^3 \times 60 \times \alpha \end{array} \right. \\ \text{metaphase: } \left\{ \begin{array}{l} \frac{V_{CO}}{dt} = (T_1 + v_3 t) \times v_2 \times \frac{22.4}{12} \times 10^3 \times 60 \times \alpha \\ \frac{V_{CO}}{dt} = T \times v_2 \times \frac{22.4}{12} \times 10^3 \times 60 \times \alpha \end{array} \right. \\ \text{anaphase: } \frac{V_{CO}}{dt} = T \times v_3 \times \frac{22.4}{12} \times 10^3 \times 60 \times \alpha \end{array} \right. \quad (21)$$

Regarding the carbon content  $\omega_{C_A}$  in the transition from the second stage to the third stage, scholars have different views and differ greatly. In actual production, it is 0.1%~0.2% or 0.2%~0.3%, or even as high as 1%~1.2%. According to the literature and relevant experience, this paper selects the transition carbon content  $\omega_{C_A} = 0.6\%$ ,

$\omega_{C_B} = 3.3\%$ . Substituting the relevant parameters in Table 1 and the derived parameters of the decarburization equation into Formula (22), the function of the amount of CO bubbles generated by the carbon-oxygen reaction in the converter molten pool to form an effective stirring gas with the blowing time is obtained, as shown in Fig.4.

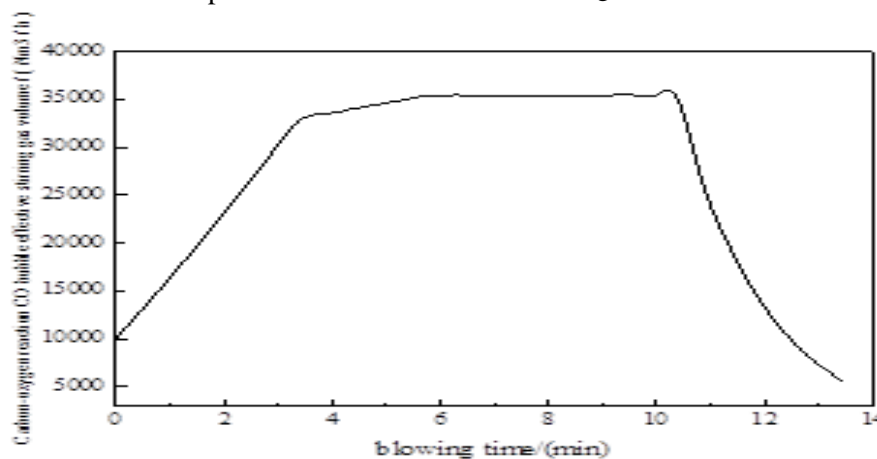


**Figure4.** Carbon-oxygen reaction CO bubble effective stirring gas volume change with blowing time.

In this paper, six different numerical simulation schemes are used to theoretically analyze the influence of molten steel velocity and flow field

distribution characteristics under the action of carbon-oxygen reaction, as shown in table 2 below.

**Table2.** Numerical simulation calculation scheme.

Scheme number	Top blowing pressure / Mpa	CO gas volume / Nm <sup>3</sup> ·h <sup>-1</sup>	bottom blowing flux / Nm <sup>3</sup> ·h <sup>-1</sup>
0	0.80	0	0
1	0.80	26700	0
2	0.80	36900	0
3	0.80	18500	0
4	0.80	26700	600
5	0.80	36900	500

### DESIGN OF CO BUBBLE PHYSICAL SIMULATION DEVICE FOR CARBON-OXYGEN REACTION

Since the CO bubbles generated by the decarburization reaction in the converter are evenly distributed throughout the molten pool, it is difficult to simulate each position separately.

This is also the reason why many metallurgical scholars have not yet carried out physical simulation studies on the changes in the flow field of the molten pool caused by the carbon-oxygen reaction. In order to simulate the process in the physical model, this study invented a patent for the method and device of carbon-oxygen reaction bubble dynamics water model test in steelmaking process. By using the method of finite element segmentation, the converter bath is divided into several small cubes, each cube node is equivalent to the CO

bubble generation point, and the structure setting and tube number selection of the gas simulation tube are carried out based on the CO simulation gas flow. The gas simulation tubes are evenly placed in the model, and the corresponding CO simulation gas volume is introduced into the gas simulation tube. The bubble generation device is constructed by the gas simulation tube uniformly placed in the model.

The physical simulation of the flow field changes caused by the stirring of the molten pool is carried out by using the stable output gas at the pores on the tube wall of the gas simulation tube, and the steel flow field dynamics simulation of each stage of the carbon oxygen reaction can be carried out respectively. The schematic diagram of the carbon-oxygen reaction bubble dynamics simulation device is shown in Fig.5.

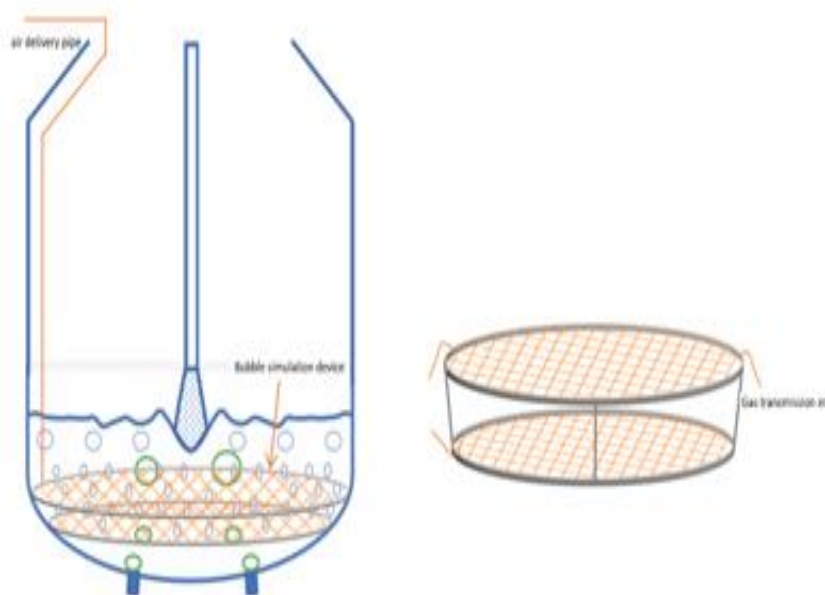


Figure 5. Schematic diagram of CO bubble physical simulation device.

(Left: integral device test diagram, right: device amplification diagram)

The theoretical instantaneous CO gas volume that can be generated can be described as in this experiment, there are four specific steps to determine the appropriate diameter, effective length and hole spacing of the trachea.

- The silicone hoses with different diameters were punched. The hole size was  $d$  and the hole spacing was  $Ld$ .
- The gas pipe is connected to the air compressor and the flow meter. The pipe body at the drilling end is immersed in water,

and the gas supply is opened to provide the maximum gas volume  $q_{max}$  of the gas pipe.

- The degree of bubble attenuation generated by the pores was directly observed. Taking the small degree of bubble attenuation as the standard, the diameter and spacing of the simulated trachea with small bubble attenuation were measured and recorded. The effective length of the simulated trachea bubble was recorded as  $L$ , and the maximum gas volume  $q_{max}$  of a single trachea was recorded as a standard simulated trachea.
- Under the condition of meeting the test requirements, taking the small size of the

simulated gas pipe as the priority principle, the appropriate number of layers of gas pipe layout and the length of the simulated gas pipe are determined. The gas pipe is arranged in a horizontal and vertical grid. According to the measured effective length of gas blowing  $L$ , the maximum gas volume  $q_{\max}$  and the maximum gas volume  $Q_{\max}$  in the

middle of decarburization, the number of simulated gas pipes  $n$  is designed. where  $n \geq (Q_{\max} / q_{\max})$ .

In this experiment,  $v < 0.2 \text{ m}\cdot\text{s}^{-1}$ ,  $v = 0.2 \sim 0.8 \text{ m}\cdot\text{s}^{-1}$  and  $v > 0.8 \text{ m}\cdot\text{s}^{-1}$  was used as the boundary value area of velocity in three regions. The flow rate statistics of different schemes are shown in Fig.6.

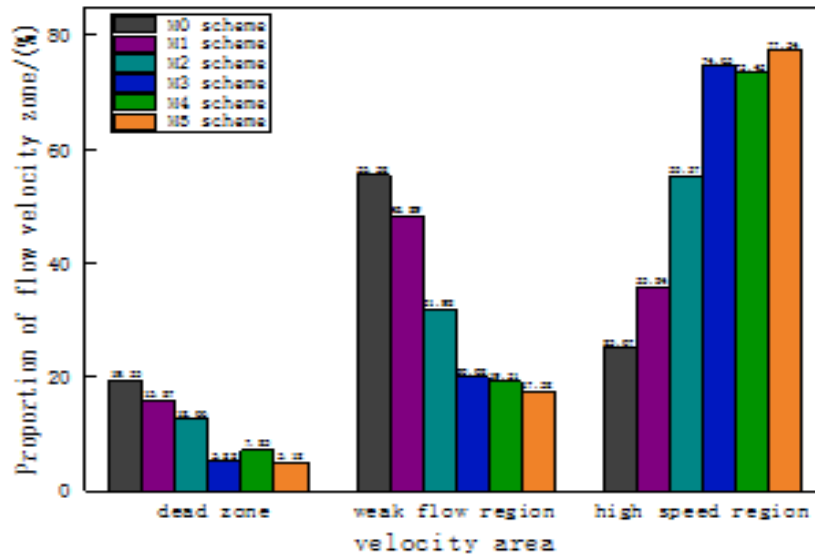


Figure6. Statistics of the proportion of molten steel flow rate area.

When there is no CO bubble stirring in scheme 0, the proportion of dead zone ( $v < 0.05 \text{ m}\cdot\text{s}^{-1}$ ) in the molten pool is 19.35%, the proportion of weak current zone is larger, and the proportion of high speed zone is smaller, which is quite different from that of carbon oxygen reaction. In the top blowing scheme of carbon-oxygen reaction simulation, in the middle stage of decarburization (scheme 3) with strong carbon-oxygen reaction, the proportion of dead zone is 5.28% and the proportion of high-speed zone is 74.65%. In the early stage of decarburization (scheme 2) the proportion of dead zone is 12.66% and the proportion of high-speed zone is 55.37%. In the end of decarburization (scheme 1), the proportion of dead zone in molten pool is 15.87% and the proportion of high-speed zone is 35.84%. From the middle to the end of decarburization, the proportion of dead zone increased by 10.59%, the proportion of high-speed zone decreased by 38.81%, and the stirring speed of molten pool decreased greatly.

### CONCLUSION

- According to the basic hypothesis setting conditions and the three-stage classical theory of decarburization, according to the prototype 8:1 scale reduction, the theoretical derivation and calculation of the parameters of the decarburization reaction kinetic

equation of the 120t converter with specific molten iron composition and blowing system were carried out. The decarburization rate equation and carbon content change function of the 120t converter in a factory were established, which laid a theoretical foundation for the research of the converter.

- According to the deduced decarburization rate equation, carbon content change function and scrap melting rate, a mathematical model of CO gas volume change for effective stirring of molten pool in the decarburization process theory of 120t converter in a factory is established, which provides a research method.
- According to the mathematical model of CO gas volume change in converter decarburization process, a CO bubble dynamic water model device for carbon-oxygen reaction was designed.

### REFERENCE

- [1] Zhang Ning, Wu Hao. Measures to improve converter gas recovery in Tang Steel New Area [J]. Metallurgical Energy, 2022, 41 (03): 45-49.
- [2] Wang Haifeng, Ping Xiaodong, Zhou Jicheng, etc. Review and Prospect of Green Development of China's Iron and Steel Industry [J]. Steel, 2022: 1-12.
- [3] Li Xiao, Peng Feng. 'Eleventh Five-Year' Review and Prospect of Steelmaking Technology



- Progress in China [J].Metallurgical Economy and Management, 2011 (06): 15-18.
- [4] RuZuodong, Zhang Yingjia, Wang Chunjiang, et al. Optimization of oxygen lance nozzle of 120t converter and its jet characteristics in steelmaking environment [J].Steelmaking, 2022,38 (04): 21-27.
- [5] Xiao Zeqiang, Zhu Miaoyong. Application of numerical simulation analysis technology in metallurgical process [M]. Beijing: Metallurgical Industry Press, 2006.
- [6] Xiao Xingguo. Fundamentals of Metallurgical Reaction Engineering [M]. Beijing Metallurgical Industry Press. 1997.
- [7] Chattopadhyay K, Isac M, Guthrie R I L. Applications of computational fluid dynamics (CFD) in iron- and steelmaking: Part 1[J].Iron-making & Steelmaking, 2010, 37(8):554-561.
- [8] Chattopadhyay K, IsacM, Guthrie R I L. Applications of computational fluid dynamics (CFD) in iron- and steelmaking: part 2[J].Iron-making & Steelmaking, 2010, 37(8):562-569.
- [9] Mazumdar D, Evans J W. Modeling of steel making Processes [M]. Boca Raton, FL: CRC Press, 2010.
- [10] Scheme and energy saving analysis of primary flue gas purification system for 120t converter [J]. Energy saving, 2023, 42 ( 02 ) : 76-78.
- [11] Dogan N, Brooks G A, Rhamdhani M A. Comprehensive model of oxygen steelmaking part 3: decarburization in impact zone[J].ISIJ International,2011,51(07):1102-1109.
- [12] Dogan N, Brooks G A, Rhamdhani M A. Comprehensive model of oxygen steelmaking part1: model development and validation [J].ISIJ International, 2011, 51(07): 1086-1092.
- [13] Dogan N,Brooks G A,Rhamdhani M A. Comprehensive model of oxygen steelmaking part 2: application of bloated droplet theory for decarburization in emulsion zone[J].ISIJ International,2011,51(07):1093-1101.
- [14] Cao Lingling. Simulation study on gas-slag-metal multiphase flow behavior in converter bath [D].Beijing University of Science and Technology, 2019.
- [15] J. H. Zong,J. K. Yoon. Theoretical interpretation of the decarburization mechanism in convective oxygen steelmaking [J]. Metallurgical Transactions B, 1990, 21B: 49-57.

**Citation:** Chen Fang, Kang Xinlei, Song Yingqian, Qin Debo, Xu Liang, Zhang Chaojie and Zhang Liqiang, "Study on the Theory and Simulation Experiment of Coal Gas Generation in Converter", *International Journal of Research Studies in Science, Engineering and Technology*, vol. 10, no.1, pp. 28-36, 2023.

**Copyright:** © 2023 Kang Xinlei, Zhang Liqiang and Song Yingqian, et al. This is an open-access article distributed under the terms of the Creative Commons Attribution License, which permits unrestricted use, distribution, and reproduction in any medium, provided the original author and source are credited.